

Nucleon-nucleon interaction and large N_c QCD

Manoj K. Banerjee, Thomas D. Cohen, and Boris A. Gelman
Department of Physics, University of Maryland, College Park, Maryland 20742-4111
 (Received 2 October 2001; published 4 March 2002)

The nature of the nonrelativistic nucleon-nucleon potential in the large- N_c limit is discussed. In particular, we address the consistency of the meson-exchange picture of nucleon interactions. It is shown that the nonrelativistic nucleon-nucleon potential extracted from the Feynmann graphs up to and including two-meson-exchange diagrams satisfies the spin-flavor counting rules of Kaplan and Savage and of Kaplan and Manohar, provided the nucleon momenta is of order N_c^0 . The key to this is a cancellation of the retardation effect of the box graphs against the contributions of the crossed-box diagram. The consistency requires including Δ as an intermediate state.

DOI: 10.1103/PhysRevC.65.034011

PACS number(s): 21.30.Cb, 11.15.Me, 11.15.Pg, 13.75.Cs

I. INTRODUCTION

One of the most fundamental problems in nuclear physics is to understand how low-energy nucleon-nucleon interactions arise from the underlying quark-gluon interactions. Unfortunately, for some time to come QCD is likely to remain computationally intractable in this regime in the sense that one will not be able to directly predict the values of low-energy nuclear physics observables by calculations based solely on the QCD Lagrangian. Nevertheless one might hope to be able to deduce some qualitative (or perhaps semiquantitative) features of nucleon-nucleon interactions from our knowledge of QCD. The known simplifications of certain aspects of QCD in the large- N_c limit could provide such a tool [1–5]. Indeed, several years ago it was proposed that the spin-flavor structure of the dominant terms in the nucleon-nucleon potential can be understood in terms of large- N_c QCD [6,7]. As we shall argue here large- N_c QCD can provide additional insights into the nature of the nucleon-nucleon force. In particular, large N_c -QCD helps us to understand both the nature of the meson-exchange picture of nucleon-nucleon interactions and the limitations of such a picture. The large- N_c perspective also sheds light on the role of the Δ resonance in nucleon-nucleon interactions. At a practical level, knowledge of the special role played by Δ in cancelling certain large contributions may prove to be useful in constructing nucleon-nucleon interactions.

The first treatment of nucleon-nucleon interactions in large- N_c QCD was done by Witten in his seminal paper on baryons in the large- N_c limit [2]. He argued that the dominant interaction between two baryons is generically of order N_c . His argument was based on consideration of diagrams such as the one in Fig. 1. It is clear that such a diagram is of order N_c —a factor of N_c^3 from combinatorics and a factor of N_c^{-2} from the coupling constants. It is straightforward to see that all quark-line-connected graphs beginning and ending with two flavor singlet combinations of N_c quarks will be $O(N_c)$ or less. However, this interaction strength of order N_c cannot represent the strength of the nucleon-nucleon scattering amplitude. In the first place, unitarity implies that the scattering amplitude does not grow without a bound as N_c goes to infinity. Second, one can consider graphs like Fig. 2,

which although disconnected at the quark level, contribute at the nucleon-nucleon level to the full interaction. It is straightforward to see that the graph in Fig. 2 is of order N_c^2 so that the interaction cannot simply go as N_c . One natural way to interpret the physics contained in the diagrams typified by Figs. 1 and 2 is to argue that they get translated at the hadronic level to contributions from nucleon-meson diagrams as in Figs. 3 and 4. In such a hadron-based picture the $O(N_c^2)$ contribution then appears as the iteration of an underlying $O(N_c)$ interaction. One key issue addressed in this paper concerns the nature of the translation from the quark-

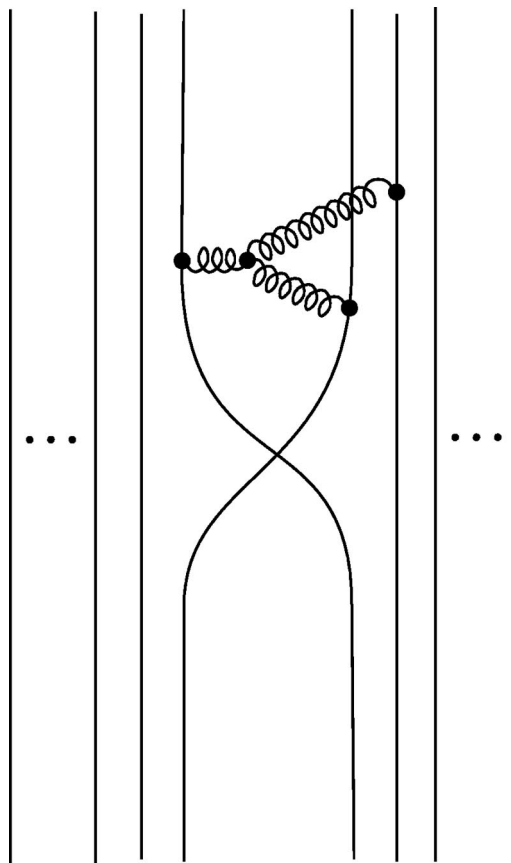
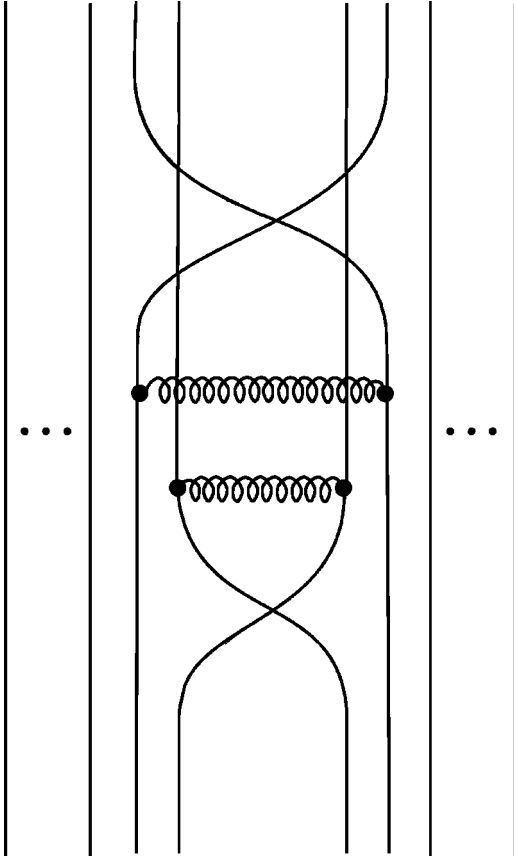


FIG. 1. A typical diagram of order N_c contributing to the nucleon-nucleon scattering in the large- N_c limit.


 FIG. 2. A typical diagram of order N_c^2 .

gluon based diagrams of Figs. 1 and 2 to the hadronic based ones of Figs. 3 and 4.

Witten [2] noted an additional difficulty of having nucleon-nucleon interaction scaling as N_c , there is no description of the scattering process, which possesses a smooth large- N_c limit if the momenta are of order unity. The basic difficulty in this case is that the kinetic energy of the nucleons is generically much smaller than the potential energy and the interplay of kinetic and potential energy, which is at the crux of scattering, cannot be independent of N_c . Witten noted that if one works in a kinematic regime with momenta of order N_c (i.e., an approach to the large- N_c limit with the nucleon velocities rather than momenta fixed), then the kinetic and potential terms are of the same order so that a smooth limit is possible. For this kinematic regime Witten suggested that the scattering process can be described using the time-dependent Hartree (TDH) approximation. It is straightforward to see that the TDH equations with fixed initial velocity have solutions that are independent of N_c . In practice, such TDH calculations have not been done in QCD and would be very difficult for systems with light quarks.

Here we wish to focus on a different limit than Witten's, i.e., on low momentum nuclear reactions. Accordingly we do not wish to let the nucleon momenta scale with N_c ; rather we will restrict our attention to the kinematic regime of nucleon momenta of order N_c^0 . As noted by Witten, in such a regime there is no smooth expression for the scattering amplitude. However, as argued by Kaplan and co-workers [6,7]

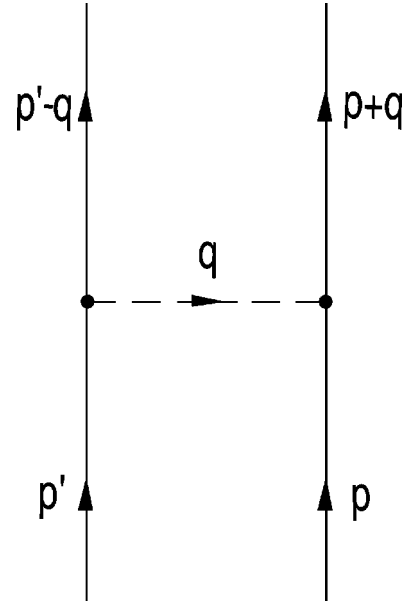


FIG. 3. A one-meson-exchange diagram contributing to the nucleon-nucleon potential; initial and final nucleons are on-shell; $p = (|\vec{p}|^2/2m_N, -\vec{p})$, $p' = (|\vec{p}'|^2/2m_N, \vec{p}')$, and $q = (q^0, \vec{q})$ are energy-momentum four-vectors flowing through the various lines.

(KSM), in this regime one may identify the nucleon-nucleon interaction from the quark-line-connected pieces as a nonrelativistic potential that has a dominant contribution of order N_c . Such a description can be interpreted on the hadronic level as a meson exchange. The one-meson-exchange potential (Fig. 3) can be as large as $O(N_c)$ since a generic baryon-meson coupling is of order $\sqrt{N_c}$ [2] and hence the large- N_c scaling at the hadronic level is consistent with the quark-gluon level. The key insight of Refs. [3–5] is that large- N_c QCD implies an approximate contracted SU(4) spin-isospin symmetry on the baryons and that this symmetry imposes constraints on the dominant parts of the potential. Thus, the dominant part of the nucleon-nucleon interaction is constrained to be contracted SU(4) symmetric, and terms that break this symmetry are suppressed by two powers of N_c . For example, the dominant $O(N_c)$ contribution to the tensor force is proportional to $\vec{\tau}_1 \cdot \vec{\tau}_2$, while the isospin independent part only contributes at order N_c^{-1} .

This paper will address a number of issues connected with the nucleon-nucleon interaction in large- N_c QCD. One central issue is the identification of the connected diagrams, such as Fig. 3, as a nonrelativistic potential (of order N_c), as was done in Refs. [6,7]. The argument for doing this is clearly heuristic and is based on the notion that large interactions must be iterated to all orders. Of course, a potential used in a Schrödinger equation is iterated to all orders. This interpretation seems to resolve in a simple manner the order N_c^2 contributions of Fig. 4; it is just one iteration of the potential (among an infinite number of possible iterations).

Unfortunately, this heuristic argument is not unique: an alternative argument would be to identify such an interaction with a kernel of a Bethe-Salpeter equation (with a strength of order N_c), which again is to be iterated to all orders. More-

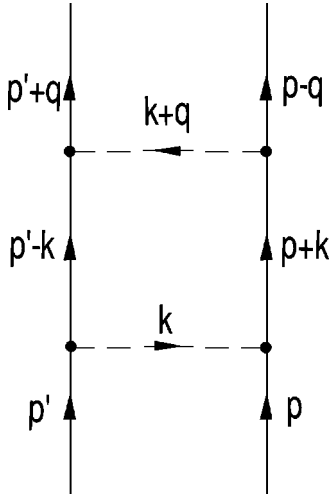


FIG. 4. A box diagram; $p = (|\vec{p}|^2/2m_N, -\vec{p})$, $p' = (|\vec{p}'|^2/2m_N, \vec{p}')$, $k = (k^0, \vec{k})$, and $q = (q^0, \vec{q})$ are energy-momentum four-vectors.

over, it is by no means clear that these are equivalent—a Bethe-Salpeter kernel of order N_c does not necessarily imply that the potential in a nonrelativistic reduction of the Bethe-Salpeter equation is of order N_c . Thus, at the fundamental level it has to be established whether large- N_c QCD is consistent with a nonrelativistic nucleon-nucleon potential of order N_c or with a Bethe-Salpeter kernel of order N_c .

A second fundamental issue in this paper is the extent to which large- N_c QCD justifies a meson-exchange picture of nucleon-nucleon interactions. A meson exchange is a natural way to understand nucleon-nucleon interactions as arising from QCD: QCD leads to the existence of colorless hadronic states—baryons and mesons—and the interactions between baryons arise from the exchange of virtual mesons. Indeed, some phenomenologically successful nucleon-nucleon potentials are based directly on a meson-exchange picture [8]. On the other hand, the argument for meson exchange dominating the nucleon-nucleon interaction is not compelling and many equally successful nucleon-nucleon potentials include only one-pion exchange treating all shorter distance effects purely phenomenologically [9]. At first sight it might seem that large- N_c arguments do not support the meson-exchange picture of nucleon-nucleon interactions. In the first place, as noted by Witten [2], baryons in the large- N_c limit behave as solitons, and when two solitons are brought close enough to interact each one distorts in the presence of the other, yielding effects that cannot be easily described in terms of meson exchange. Indeed Witten's prescription for scattering for momenta of order N_c , TDH, necessarily builds in these non-meson-exchange-type effects; the clusters of N_c quarks that interact in TDH are *not* simply the Hartree wave functions for two nucleons.

There is a second reason why one might suspect that large- N_c QCD does not justify a meson-exchange point of view for nucleon-nucleon interactions. The meson-exchange picture does not imply only single meson exchanges but two or more meson exchanges as well. Consider, the large- N_c scaling of a generic two-meson-exchange process. Some

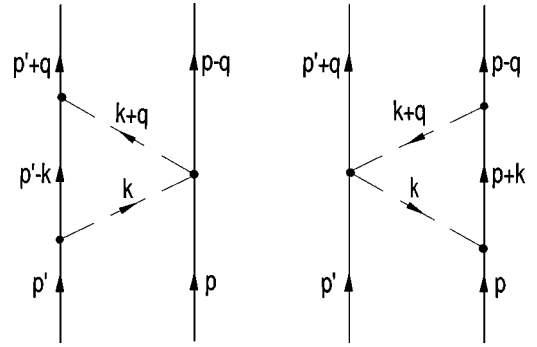


FIG. 5. Triangle diagrams; $p = (|\vec{p}|^2/2m_N, -\vec{p})$, $p' = (|\vec{p}'|^2/2m_N, \vec{p}')$, $k = (k^0, \vec{k})$, and $q = (q^0, \vec{q})$ are energy-momentum four-vectors.

typical diagrams contributing to the potential are shown in Fig. 5, in which two exchange mesons are coupled to one of the nucleons at a single vertex. Such diagrams are generically of order N_c since the coupling of the meson current to a nucleon is of order N_c^0 [2]; the additional power of N_c comes from two nucleon-meson vertices (each of which contributes $N_c^{1/2}$). Thus, these diagrams are consistent with the previously deduced large- N_c scaling behavior of the potential. However, if one considers a generic crossed-box diagram as shown in Fig. 6, one encounters an inconsistency. Since, the nucleon-meson coupling is generically of order $\sqrt{N_c}$, the diagram in Fig. 6 is of order N_c^2 . This scaling, however, violates the proposed large- N_c scaling of the nucleon-nucleon potential (which is supposed to go as N_c). Clearly, three and more meson-exchange diagrams will yield ever-larger inconsistencies.

This paper will also address another central issue in nucleon-nucleon physics, namely, the role of the Δ resonance in intermediate states. As is well known, the Δ resonance has a low excitation energy for large N_c (with $m_\Delta - m_N \sim N_c^{-1}$) [4,10]. Moreover, the inclusion of virtual Δ 's is known to be essential to ensure the consistency of large- N_c predictions for hadronic processes and its inclusion is neces-

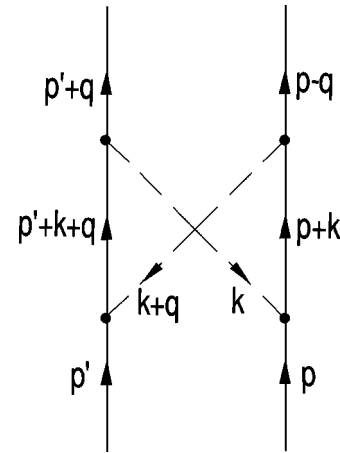


FIG. 6. A crossed-box diagram; $p = (|\vec{p}|^2/2m_N, -\vec{p})$, $p' = (|\vec{p}'|^2/2m_N, \vec{p}')$, $k = (k^0, \vec{k})$, and $q = (q^0, \vec{q})$ are energy-momentum four-vectors.

TABLE I. Nonrelativistic scalar and pseudoscalar meson-baryon couplings. The ground state baryons B belong to an irreducible representation $I=J$.

	Scalars		Pseudoscalars	
	$I=0$	$I=1$	$I=0$	$I=1$
Meson	f_0	a_0	η	π
Meson-baryon coupling	$B^\dagger B \phi$	$B^\dagger I^a B \phi^a$	$B^\dagger J^i B \partial^j \phi$	$B^\dagger X^{ia} B \partial^j \phi^a$
Scaling of the coupling	$\sqrt{N_c}$	$(\sqrt{N_c})^{-1}$	$(\sqrt{N_c})^{-1}$	$\sqrt{N_c}$
Spin-flavor term	V_0^0	V_0^1	V_T^0	V_T^1
KSM scaling	N_c	N_c^{-1}	N_c^{-1}	N_c

sary for the contracted SU(4) spin-flavor structure of baryons to be manifest. Thus, one might expect that virtual Δ 's will also play a key role in nucleon-nucleon reactions in the large- N_c limit.

In this paper we will show that the following picture is consistent with large- N_c QCD:

(i) The nucleon-nucleon interaction can be described by a potential of order N_c but *not* by a Bethe-Salpeter kernel of order N_c .

(ii) The meson-exchange picture can be used consistently to describe nucleon-nucleon interactions for momenta of order N_c^0 .

(iii) The meson-exchange picture of the nucleon-nucleon potential (of order N_c) breaks down for momenta of order N_c .

(iv) The leading order nucleon-nucleon potential is symmetric under contracted SU(4) with corrections down by two powers in N_c yielding the spin-flavor structure of Refs. [6,7].

(v) The contracted SU(4) structure implies a central role for intermediate states containing Δ 's.

The basic strategy of this paper is to assume that the picture outlined above is correct and then to show that it does not lead to any inconsistencies up to and including two-meson-exchange potentials. The key difficulty that must be addressed is the problem of the crossed-box graphs mentioned above: If point (ii) is correct then they must be included; however, they generically contribute to the potential at order N_c^2 , which exceeds the potential's supposed order N_c scale from point (i). More generally they lead to contributions that are inconsistent with the spin-flavor structure of Refs. [6,7]. However, as we will show, all contributions from the crossed-box graphs that are inconsistent with the spin-flavor structure of Refs. [6,7] are canceled by contributions coming from the retardation effects in the box graphs. While it has long been known that such a cancellation occurs for scalar isoscalar mesons between retardation effects in the box graph and the crossed-box graph [11], it has not been previously shown that such cancellations are far more general and protect the large- N_c structure of the nucleon-nucleon potential including the hierarchy of large and small contributions in terms of spin and isospin. It will also be shown that such a cancellation does not occur if Δ intermediate states are excluded or if the momenta of the nucleons is of order N_c .

II. REVIEW OF THE SU(4) CONTRACTED SYMMETRY

The baryon sector of large- N_c QCD exhibits an approximate SU(4) contracted light quark spin-flavor symmetry

[3–5]. The contracted SU(4) algebra is

$$\begin{aligned}
 [J^i, J^j] &= i\epsilon_{ijk} J^k, & [I^a, I^b] &= i\epsilon_{abc} I^c, & [J^i, I^a] &= 0, \\
 [J^i, X_0^{jb}] &= i\epsilon_{ijk} X_0^{kb}, & [I^a, X_0^{jb}] &= i\epsilon_{abc} X_0^{jc}, & [X_0^{ia}, X_0^{jb}] &= 0,
 \end{aligned} \tag{1}$$

where $i, a = 1, 2, 3$ are spin and isospin indices.

In large- N_c two-flavor QCD, baryons belong to the infinite-dimensional irreducible representation of the contracted SU(4) algebra with $I=J=1/2, 3/2, 5/2, \dots$ [3–5]. For $N_c=3$ the $I=J=1/2$ and $I=J=3/2$ states are identified with the nucleon and Δ . Other states are presumably a large- N_c artifact. The meson-baryon couplings connecting the states with different spin and isospin are given in terms of the matrix elements of X^{ia} , which is defined by its matrix elements between baryon states [e.g., Eq. (4)]. This operator is equal to X_0^{ia} at leading order in the $1/N_c$ expansion. As shown in Ref. [4], the next-to-leading order term is proportional to X_0^{ia}

$$X^{ia} = \left(1 + \frac{\alpha}{N_c}\right) X_0^{ia} + O(1/N_c^2), \tag{2}$$

where α is a constant independent of the spin and isospin indices. As a result, the spin-flavor operators X^{ia} commute up to $O(N_c^{-2})$ corrections

$$[X^{ia}, X^{jb}] = O\left(\frac{1}{N_c^2}\right). \tag{3}$$

Meson-baryon couplings satisfying the contracted spin-flavor symmetry are listed in the third row of Tables I and II. These couplings are obtained from the nonrelativistic reduction of the corresponding covariant Yukawa couplings with corrections suppressed by $1/N_c$. The matrix elements of the X_0^{ia} generators between the baryon states are given in terms of the Clebsch-Gordan coefficients by [4]

$$\begin{aligned}
 \langle I' I'_3, J' J'_3 | X_0^{ia} | I I_3, J J_3 \rangle &= \sqrt{\frac{(2J+1)}{(2J'+1)}} \langle J', J'_3 | J J_3; 1i \rangle \\
 &\quad \times \langle I', I'_3 | I I_3; 1a \rangle,
 \end{aligned} \tag{4}$$

where only spin and isospin labels of the baryon states are shown explicitly.

TABLE II. Nonrelativistic vectors and pseudovector meson-baryon couplings. The ground state baryons B belong to an irreducible representation $I=J$.

	Vectors				Pseudovectors	
	$I=0$	$I=0$	$I=1$	$I=1$	$I=0$	$I=1$
Meson	ω^t	$\vec{\omega}$	ρ^t	$\vec{\rho}$	\vec{f}_1	\vec{a}_1
Meson-baryon coupling	$B^\dagger B V^t$	$B^\dagger \epsilon_{ijk} J^k B \partial^i V^j$	$B^\dagger I^a B V^{ta}$	$B^\dagger \epsilon_{ijk} X^{ka} B \partial^i V^j$	$B^\dagger J^i B A^i$	$B^\dagger X^{ia} B A^{ia}$
Scaling	$\sqrt{N_c}$	$(\sqrt{N_c})^{-1}$	$(\sqrt{N_c})^{-1}$	$\sqrt{N_c}$	$(\sqrt{N_c})^{-1}$	$\sqrt{N_c}$
Spin-flavor term	V_0^0	V_T^0	V_0^1	V_T^1	V_σ^0	V_σ^1
KSM scaling	N_c	N_c^{-1}	N_c^{-1}	N_c	N_c^{-1}	N_c

We will need to know the matrix elements of the anticommutators between the nucleon states. When restricting attention to nucleon initial and final states one can easily deduce that

$$\{J^i, X^{ja}\}_{N'N} = \frac{1}{2} \delta^{ij} I^a + O\left(\frac{1}{N_c^2}\right),$$

$$\{I^a, X^{ib}\}_{N'N} = \frac{1}{2} \delta^{ab} J^i + O\left(\frac{1}{N_c^2}\right), \quad (5)$$

where we have used the fact that J^i and I^a only take nucleons into nucleons. The $O(1/N_c)$ corrections in Eq. (5) vanish due to the fact that the constant α in Eq. (2) is independent of the spin and isospin.

The large- N_c scaling of the baryon matrix elements have been analyzed in Refs. [4,5]. Since a general one-quark operator (e.g., axial vector current) can couple to any of the N_c quarks in a baryon, its matrix elements between ground state baryons are of order N_c (providing the cancellation between different quark-line insertions does not occur). The operators with spin-flavor structure given by $\mathbf{1}$ and X^{ia} behave in this leading fashion [4]. On the other hand, currents containing only J^i and I^a are of order N_c^0 . Heuristically, the reason is that for baryons with $J=I=1/2, 3/2, \dots$ only one out of N_c quarks carry the spin and isospin quantum numbers of the state. The large- N_c scaling of a meson-baryon coupling is obtained by dividing the corresponding current matrix element by the meson decay constant, which is of order $N_c^{-1/2}$. Hence, the meson-baryon couplings containing spin-flavor operators $\mathbf{1}$ or X^{ia} are of order $N_c^{1/2}$. Examples of such leading couplings are the couplings of f_0 and π mesons to baryons. In addition, the time component of ω (ω^t) and spatial components of ρ ($\vec{\rho}$) and a_1 (\vec{a}_1) couple to the baryons with a strength proportional to $N_c^{1/2}$. Couplings containing J^i and I^a are of order $N_c^{-1/2}$. The examples include the couplings of a_0 and η , spatial components of ω and f_1 ($\vec{\omega}$ and \vec{f}_1), and the time component of ρ (ρ^t). These counting rules are listed in the fourth row of Tables I and II.

Similarly, the spin-flavor structure of the nonrelativistic nucleon-nucleon potential can be analyzed in the large- N_c QCD. The general form of this potential is

$$V_{NN} = V_0^0 + V_\sigma^0 \vec{\sigma}_{(1)} \cdot \vec{\sigma}_{(2)} + V_T^0 S_{12} + V_{LS}^0 \vec{L} \cdot \vec{S} + V_Q^0 Q_{12} + (V_1^0 + V_\sigma^1 \vec{\sigma}_{(1)} \cdot \vec{\sigma}_{(2)} + V_T^1 S_{12} + V_{LS}^1 \vec{L} \cdot \vec{S} + V_Q^1 Q_{12}) \vec{\tau}_{(1)} \cdot \vec{\tau}_{(2)}, \quad (6)$$

where

$$S_{12} = 3 \vec{\sigma}_{(1)} \cdot \hat{r} \vec{\sigma}_{(2)} \cdot \hat{r} - \vec{\sigma}_{(1)} \cdot \vec{\sigma}_{(2)},$$

$$Q_{12} = \frac{1}{2} \{ \vec{\sigma}_{(1)} \cdot \vec{L}, \vec{\sigma}_{(2)} \cdot \vec{L} \}, \quad (7)$$

where \vec{L} and \vec{S} are the total orbital and spin angular momenta of the system of two nucleons. The operators in Eq. (6) multiplying the position and velocity dependent functions $V_n^{1,2}$ ($n=0, \sigma, T, LS, Q$) are referred to as the central, spin-spin, tensor, spin-orbit, and quadratic spin-orbit components of the nucleon-nucleon potential in the isosinglet and isotrip-let channels.

In Refs. [6,7], the large- N_c scaling of functions $V_n^{1,2}$ was analyzed using the spin-flavor counting rules of the generators of the contracted SU(4). The analysis is based on two assumptions. One is that the nucleon-nucleon interaction can be described by a Hartree Hamiltonian, which can be written as a sum of operators with a particular spin-flavor structure satisfying the large- N_c scaling rules of the contracted SU(4) symmetry. In addition, the authors implicitly assumed that the Hartree picture leads to a potential of order N_c for momenta of order one. At the hadronic level, the latter assumption is essentially equivalent to a one-meson-exchange picture of the potential. Based on the above assumptions, the following counting rules were obtained in Refs. [6,7]:

$$V_0^0 \sim V_\sigma^1 \sim V_T^1 \sim N_c, \quad V_0^1 \sim V_\sigma^0 \sim V_T^0 \sim \frac{1}{N_c}. \quad (8)$$

In addition, the spin-orbit and quadratic spin-orbit components suppressed by $1/m_B \sim 1/N_c$ (m_B is a baryon mass) are of order $1/N_c^2$. The scaling rules in Eq. (8) will be referred to as KSM counting rules.

It is easy to see how the counting rules in Eq. (8) arise from the large- N_c scaling of the meson-baryon couplings at the one-meson-exchange level. At this level, a given term in the potential, (6) scales as the square of the corresponding coupling constant. Since, for example, the isoscalar central

potential at leading order gets contributions from f_0 exchange, it is of order $(\sqrt{N_c})^2 = N_c$. Similarly, the one-pion exchange contributes to the leading part of the isovector tensor term, which, therefore, scales as $(\sqrt{N_c})^2 = N_c$. On the other hand, the isoscalar tensor potential V_T^0 is of order N_c^{-1} since its leading contribution is from one- η exchange. The leading contributions at the one-meson-exchange level are shown in the fifth row of Tables I and II; the N_c scaling of these contributions are shown in the last row of Tables I and II. We will show that the nucleon-nucleon potential is consistent with KSM counting rules, Eq. (8), up to and including two-meson-exchange contributions.

III. TWO-MESON-EXCHANGE CONTRIBUTIONS

The Feynmann diagrams contributing at the two-meson-exchange level are shown in Figs. 4, 6, and 5—the box, the crossed-box, and the triangle graphs. In these diagrams the initial and final nucleons are on-mass-shell. This condition is necessary if the diagrams are used to derive the nucleon-nucleon potential. The baryon energy-momentum relation is treated nonrelativistically with the baryon propagators having the following form:

$$\frac{i}{k^0 - |\vec{k}|^2/2m_B + i\epsilon} \left[1 + O\left(\frac{1}{N_c}\right) \right], \quad (9)$$

where k^0 and \vec{k} are the energy and the momentum of an intermediate baryon with mass m_B . In practice, $m_B = m_N$

+ $O(1/N_c)$ (m_N is the nucleon mass) for the ground state baryons with $I = J = 1/2, 3/2, 5/2, \dots$. Relativistic effects are suppressed by $1/m_B \sim N_c^{-1}$. The mesons are treated in a fully relativistic form. The meson-baryon vertices are, in general, momentum and energy dependent. Note, the time and spatial components of ω and ρ have different couplings at leading nonrelativistic order (Tables I and II). In addition, the spin-flavor structure of ω^t coupling is identical to that of f_0 (or σ). Similarly, ρ^t and a_0 couplings have identical spin-flavor structure.

A two-meson-exchange diagram may contain a piece that is equal to one iteration of the potential. These contributions will be included when solving the Schrödinger equation and must be excluded from the nucleon-nucleon potential to avoid double counting. This can be illustrated using the two-scalar-exchange diagrams.

The contribution to the nucleon-nucleon potential from a one-scalar exchange, Fig. 3, with point couplings is given by

$$V_{f_0}(\vec{q}) = \frac{g_{f_0}^2}{(q^0)^2 - |\vec{q}|^2 - m_{f_0}^2} = \frac{-g_{f_0}^2}{|\vec{q}|^2 + m_{f_0}^2} [1 + O(1/N_c^2)], \quad (10)$$

where $m_{f_0}[O(N_c^0)]$ is the mass of the f_0 meson and the coupling constant g_{f_0} is of order $\sqrt{N_c}$ (Table I). Note that $(q^0)^2$ can be neglected since q^0 is of order N_c^{-1} .

Similarly, the contribution of the two-scalar-exchange box diagram, Fig. 4, to the scattering amplitude \mathcal{M} is

$$i\mathcal{M}_{\square} = \int \frac{d^3k}{(2\pi)^3} \int \frac{dk^0}{2\pi} \frac{g_{f_0}^4}{[(k^0)^2 - |\vec{k}|^2 - m_{f_0}^2][(k^0 + q^0)^2 - |\vec{k} + \vec{q}|^2 - m_{f_0}^2]} \times \frac{1}{(k^0 + |\vec{p}|^2/2m_B - |\vec{p} - \vec{k}|^2/2m_B)(-k^0 + |\vec{p}|^2/2m_B - |\vec{p} - \vec{k}|^2/2m_B)}. \quad (11)$$

It is convenient to first perform the k^0 integral. There are two classes of poles in the complex k^0 plane, namely, from the baryon and meson propagators. It is easy to see that the baryon poles in Eq. (11) are on the opposite side of the real k^0 axis. By closing the integration contour in the upper or lower complex plane only one of these baryon poles will contribute to \mathcal{M}_{\square} . Closing the contour in the upper plane we get for the baryon pole contribution,

$$i\mathcal{M}_{\square}^B = \int \frac{d^3k}{(2\pi)^3} \frac{ig_{f_0}^4}{(|\vec{k}|^2 + m_{f_0}^2)(|\vec{k} + \vec{q}|^2 + m_{f_0}^2)(|\vec{p}|^2/m_B - |\vec{p} - \vec{k}|^2/m_B)} \left[1 + O\left(\frac{1}{N_c}\right) \right], \quad (12)$$

where, in addition to $q^0 \sim N_c^{-1}$, the position of the baryon pole, $k_B^0 = (|\vec{p}|^2 - |\vec{p} - \vec{k}|^2)/2m_B$, is neglected when the meson propagators are evaluated. However, the position of the baryon pole is of leading order when the other baryon propagator is evaluated. As will become clear, this value of a baryon propagator is identical to the nonrelativistic Green function in the Lippman-Schwinger equation for the scattering amplitude.

The baryon pole contribution \mathcal{M}_{\square}^B should be compared with one iterate of the Lippman-Schwinger equation (in the center-of-mass frame),

$$T(\vec{p}, \vec{p} + \vec{q}) = -V(\vec{q}) + \int \frac{d^3k}{(2\pi)^3} V(-\vec{k}) G_0(\vec{k}) T(\vec{p} - \vec{k}, \vec{p} + \vec{q}), \quad (13)$$

where the nonrelativistic baryon Green function is given by

$$G_0(\vec{k}) \equiv \frac{1}{(|\vec{p}-\vec{k}|^2 - |\vec{p}|^2)/m_B + i\epsilon}. \quad (14)$$

The first term in Eq. (13) corresponds to a potential at the one-meson exchange level. For the one-scalar exchange this potential is given in Eq. (10). Iterations of the Lippman-Schwinger equation lead to

$$T(\vec{p}, \vec{p} + \vec{q}) = -V(\vec{q}) + \int \frac{d^3k}{(2\pi)^3} V(-\vec{k}) G_0(\vec{k}) V(\vec{k} + \vec{q}) - \int \frac{d^3k}{(2\pi)^3} \int \frac{d^3k'}{(2\pi)^3} V(-\vec{k}) G_0(\vec{k}) V(\vec{k} + \vec{k}') G_0(\vec{k}') V(\vec{q} - \vec{k}') + \dots, \quad (15)$$

where the ellipsis indicates higher-order iterations. For the two-scalar exchange, the first iteration of the potential in Eq. (10) is

$$\int \frac{d^3k}{(2\pi)^3} V_{f_0}(-\vec{k}) G_0(\vec{k}) V_{f_0}(\vec{k} + \vec{q}) = \int \frac{d^3k}{(2\pi)^3} \frac{g_{f_0}^4}{(|\vec{k}|^2 + m_{f_0}^2)(|\vec{k} + \vec{q}|^2 + m_{f_0}^2)(|\vec{p} - \vec{k}|^2/m_B - |\vec{p}|^2/m_B)}, \quad (16)$$

which is exactly equal to the baryon pole contribution \mathcal{M}_{\square}^B [Eq. (12)] evaluated with the nonrelativistic baryon propagator, Eq. (9). Thus, the baryon pole contribution of the two-scalar box diagram should not be included in the nucleon-nucleon potential. Note, that the equality holds only if the nonrelativistic baryon propagator is used to evaluate \mathcal{M}_{\square}^B .

The remaining contribution to \mathcal{M}_{\square} is from the meson poles. This contribution is often referred to as the retardation effect since it is absent when using a static potential. The retardation effect for two-scalar exchange is of order N_c^2 (see Table I), i.e., it is larger than allowed by KSM counting rules, Eq. (8). Hence, for the two-scalar-exchange diagrams to be consistent with the counting rules, the retardation effect has to be canceled by the crossed-box diagram. The key issue is whether this cancellation indeed happens.

The baryon pole contribution in the box diagram has been discussed for the two-scalar exchange with point couplings. In fact, it can easily be generalized for any two-meson exchange with general vertex functions. Indeed, the above proof that the baryon pole contribution to the box diagram is one iterate of the potential rests only on the nonrelativistic form of the two-baryon propagators and the direction of the loop momenta and energy flow through the baryon lines. Neither the spin-flavor structure nor the vertex functions can

change the position of the baryon poles. Thus, the baryon poles from any two-meson box diagrams do not contribute to the nucleon-nucleon potential.

We have shown so far that the baryon pole contributions from the two-meson box diagrams should not be included in the nucleon-nucleon potential. However, the retardation effect and the crossed-box contribution can each be larger than allowed by the KSM counting rules. For example, the retardation effect and crossed-box diagrams corresponding to the two-pion exchange are each of order N_c^2 . Moreover, the two-meson-exchange diagrams, in general, can contribute to different spin-flavor structures in the nucleon-nucleon potential, Eq. (6). As a result, these contributions considered separately may violate the KSM counting rules of the subleading $O(N_c^{-1})$ terms in the potential. For example, two-pion-exchange box and crossed-box diagrams (each of order N_c^2) contribute not only to V_T^1 but among others to the isosinglet tensor force V_T^0 as well. The latter, however, should be of order N_c^{-1} according to Eq. (8). Fortunately, as will be shown below, the retardation effects cancel against the crossed-box diagram contributions in all such cases.

A cancellation between the retardation effect and the crossed box is well known for the two-scalar-exchange diagrams [11]. The meson pole contribution to \mathcal{M}_{\square} , Eq. (11), is

$$\begin{aligned} \mathcal{M}_{\square}^{ret} &= \int \frac{d^3k}{(2\pi)^3} \int \frac{dk^0}{2\pi} 2 \operatorname{Im} \left[\frac{g_{f_0}^4}{[(k^0)^2 - |\vec{k}|^2 - m_{f_0}^2][(k^0 + q^0)^2 - |\vec{k} + \vec{q}|^2 - m_{f_0}^2]} \right] \\ &\quad \times \operatorname{P} \left[\frac{1}{(k^0 + |\vec{p}|^2/2m_B - |\vec{p} - \vec{k}|^2/2m_B)(-k^0 + |\vec{p}|^2/2m_B - |\vec{p} - \vec{k}|^2/2m_B)} \right] \\ &= \int \frac{d^3k}{(2\pi)^3} \frac{g_{f_0}^4}{|\vec{k} + \vec{q}|^2 - |\vec{k}|^2} \left(\frac{1}{2(|\vec{k}|^2 + m_{f_0}^2)^{3/2}} - \frac{1}{2(|\vec{k} + \vec{q}|^2 + m_{f_0}^2)^{3/2}} \right) \left[1 + O\left(\frac{1}{N_c}\right) \right], \end{aligned} \quad (17)$$

where in the second step we have again neglected terms in the denominators suppressed by $1/m_B \sim 1/N_c$ including the energy q^0 ; the symbol P indicates principle value.

The contribution to the scattering amplitude from the two-meson crossed-box diagram, Fig. 6, is

$$i\mathcal{M}_X = \int \frac{d^3k}{(2\pi)^3} \int \frac{dk^0}{2\pi} \frac{g_{f_0}^4}{[(k^0)^2 - |\vec{k}|^2 - m_{f_0}^2][(k^0 + q^0)^2 - |\vec{k} + \vec{q}|^2 - m_{f_0}^2]} \times \frac{1}{(k^0 + q^0 + |\vec{p}|^2/2m_B - |\vec{p} + \vec{k} + \vec{q}|^2/2m_B)(k^0 + |\vec{p}|^2/2m_B - |\vec{p} - \vec{k}|^2/2m_B)}. \quad (18)$$

Note, the baryon poles are now on the same side of the real axis in the k^0 complex plane. Hence, they do not contribute to \mathcal{M}_X . The only nonvanishing contribution is from the meson poles,

$$\begin{aligned} \mathcal{M}_X &= \int \frac{d^3k}{(2\pi)^3} \int \frac{dk^0}{2\pi} 2\text{Im} \left[\frac{g_{f_0}^4}{[(k^0)^2 - |\vec{k}|^2 - m_{f_0}^2][(k^0 + q^0)^2 - |\vec{k} + \vec{q}|^2 - m_{f_0}^2]} \right] \\ &\times \text{P} \left[\frac{1}{(k^0 + q^0 + |\vec{p}|^2/2m_B - |\vec{p} + \vec{k} + \vec{q}|^2/2m_B)(k^0 + |\vec{p}|^2/2m_B - |\vec{p} - \vec{k}|^2/2m_B)} \right] \\ &= - \int \frac{d^3k}{(2\pi)^3} \frac{g_{f_0}^4}{|\vec{k} + \vec{q}|^2 - |\vec{k}|^2} \left(\frac{1}{2(|\vec{k}|^2 + m_{f_0}^2)^{3/2}} - \frac{1}{2(|\vec{k} + \vec{q}|^2 + m_{f_0}^2)^{3/2}} \right) \left[1 + \mathcal{O}\left(\frac{1}{N_c}\right) \right], \end{aligned} \quad (19)$$

where the same approximations as in Eq. (17) were made. As evident from Eqs. (17) and (19), the retardation effect and crossed-box diagram contribution for the two-scalar exchange cancel out up to corrections of order N_c^{-1} ,

$$\mathcal{M}_{\square}^{\text{ret}} + \mathcal{M}_X = \mathcal{O}\left(\frac{1}{N_c}\right). \quad (20)$$

It is important to stress, however, that the above cancellation does not occur when the nucleon momenta are of order N_c since for the momenta of order N_c the baryon propagators evaluated at the meson poles are different [as can be seen from Eqs. (17) and (19)]. Consequently, for the momenta of order N_c , the nucleon-nucleon interaction cannot be interpreted as a simple meson-exchange picture consistent with the KSM counting rules, Eq. (8). As will be shown below, the cancellation in Eq. (20) is far more general. In fact, it occurs for all two-meson-exchange graphs provided the nucleon momenta are of order N_c^0 and the meson-baryon couplings are contracted SU(4) symmetric. Let us consider a general box and crossed-box diagram containing any pair of intermediate mesons.

We will use Greek symbols to indicate an exchanged meson, e.g., $\alpha = f_0, \rho, \pi, \dots$. A given graph contains four vertex functions, one for each meson-baryon coupling. The product of these four functions will be denoted by $\tilde{V}_{\alpha\beta}(k^0, \vec{k}, q^0, \vec{q})$. The function $\tilde{V}_{\alpha\beta}(k^0, \vec{k}, q^0, \vec{q})$ does not contain spin-flavor matrices of the corresponding meson-baryon couplings, which will be written explicitly. It is clear that $\tilde{V}_{\alpha\beta} = \tilde{V}_{\beta\alpha}$. To simplify the formulas we combine the product of $\tilde{V}_{\alpha\beta}(k^0, \vec{k}, q^0, \vec{q})$ and two-meson propagators into a single energy-momentum dependent function $V_{\alpha\beta}(k^0, \vec{k}, q^0, \vec{q})$ defined by

$$V_{\alpha\beta}(k^0, \vec{k}, q^0, \vec{q}) \equiv \frac{\tilde{V}_{\alpha\beta}(k^0, \vec{k}, q^0, \vec{q})}{[(k^0)^2 - |\vec{k}|^2 - m_{\alpha}^2][(k^0 + q^0)^2 - |\vec{k} + \vec{q}|^2 - m_{\beta}^2]}, \quad (21)$$

where m_{α} and m_{β} are the masses of the α and β mesons. The above-defined function is symmetric under the interchange of the exchanged mesons, $V_{\alpha\beta} = V_{\beta\alpha}$. The analytic structure of $V_{\alpha\beta}(k^0, \vec{k}, q^0, \vec{q})$ as a function of a complex variable k^0 determines the retardation effects of the box graphs and the contribution of the crossed-box diagrams.

The spin-flavor structure of the meson-baryon vertices will be denoted by $\Gamma_{\alpha(n)}^A(\vec{k})$, where a superscript A specifies the spin-flavor indices and subscript $n=1,2$ indicates to which of the two baryon lines a meson couples. The momentum dependence arises in the case of derivatively coupled mesons such as pions. The product of the two $\Gamma_{\alpha(n)}^A(\vec{k})$ structures at two ends of the same meson propagator are constrained by the spin and isospin of the exchanged meson. To enforce these constraints in the product $\Gamma_{\alpha(1)}^A(\vec{k})\Gamma_{\alpha(2)}^B(-\vec{k})$, we introduce a symbol C_{AB}^{α} . For example, in the case when the exchanged meson is a pion, the above product takes the form

$$\begin{aligned} C_{AB}^{\pi} \Gamma_{\pi(1)}^A(\vec{k}) \Gamma_{\pi(2)}^B(-\vec{k}) &= -\delta^{ij} \delta^{mn} \delta^{ab} k^j k^n X_{(1)}^{ia} X_{(2)}^{mb} \\ &= -k^i k^m X_{(1)}^{ia} X_{(2)}^{ma}, \end{aligned} \quad (22)$$

where the contracted SU(4) pion-baryon coupling is used.

Using the above notation a contribution from a general box graph, Fig. 4, has the following form:

$$i\mathcal{M}_\square = g_\alpha^2 g_\beta^2 \int \frac{d^3k}{(2\pi)^3} \int \frac{dk^0}{2\pi} \frac{V_{\alpha\beta}(k^0, \vec{k}, q^0, \vec{q}) C_{AB}^\alpha C_{CD}^\beta \Gamma_{\alpha(1)}^A(\vec{k}) \Gamma_{\beta(1)}^C(-[\vec{k}+\vec{q}]) \Gamma_{\alpha(2)}^B(-\vec{k}) \Gamma_{\beta(2)}^D(\vec{k}+\vec{q})}{(k^0 + |\vec{p}|^2/2m_B - |\vec{p}-\vec{k}|^2/2m_B)(-k^0 + |\vec{p}|^2/2m_B - |\vec{p}-\vec{k}|^2/2m_B)}, \quad (23)$$

where g_α and g_β are the corresponding coupling constants, and the momenta directions are shown in Fig. 4. The crossed box, Fig. 6, has a similar expression with the last two Γ 's interchanged,

$$i\mathcal{M}_X = g_\alpha^2 g_\beta^2 \int \frac{d^3k}{(2\pi)^3} \int \frac{dk^0}{2\pi} \frac{V_{\alpha\beta}(k^0, \vec{k}, q^0, \vec{q}) C_{AB}^\alpha C_{CD}^\beta \Gamma_{\alpha(1)}^A(\vec{k}) \Gamma_{\beta(1)}^C(-[\vec{k}+\vec{q}]) \Gamma_{\beta(2)}^D(\vec{k}+\vec{q}) \Gamma_{\alpha(2)}^B(-\vec{k})}{(k^0 + q^0 + |\vec{p}|^2/2m_B - |\vec{p}+\vec{k}+\vec{q}|^2/2m_B)(k^0 + |\vec{p}|^2/2m_B - |\vec{p}-\vec{k}|^2/2m_B)}. \quad (24)$$

Note the difference in the baryon propagators relative to Eq. (23) due to the difference in the momentum flow.

As was previously shown, the baryon pole contribution to the box graph is the first iterate of the Lippman-Schwinger equation while these poles do not contribute to the crossed-box graph at this order. As in the case of the scalar exchange, the k^0 integration in Eqs. (23) and (24) can be performed via contour integration. Whatever the explicit form of the function $V_{\alpha\beta}(k^0, \vec{k}, q^0, \vec{q})$ its contribution to the k^0 integral is given by its imaginary part. The important point is that the same function appears in \mathcal{M}_\square and \mathcal{M}_X . Since the intermediate baryons cannot go on-shell at the meson singularities their contribution equals the principal values of their propagators.

The retardation effect of the box diagram is

$$\begin{aligned} \mathcal{M}_\square^{ret} &= g_\alpha^2 g_\beta^2 \int \frac{d^3k}{(2\pi)^3} \int \frac{dk^0}{2\pi} 2 \operatorname{Im}[V_{\alpha\beta}(k^0, \vec{k}, q^0, \vec{q})] C_{AB}^\alpha C_{CD}^\beta \Gamma_{\alpha(1)}^A(\vec{k}) \Gamma_{\beta(1)}^C(-\vec{k}-\vec{q}) \Gamma_{\alpha(2)}^B(-\vec{k}) \Gamma_{\beta(2)}^D(\vec{k}+\vec{q}) \\ &\quad \times \mathcal{P} \left[\frac{1}{(k^0 + |\vec{p}|^2/2m_B - |\vec{p}-\vec{k}|^2/2m_B)} \frac{1}{(-k^0 + |\vec{p}|^2/2m_B - |\vec{p}-\vec{k}|^2/2m_B)} \right] \\ &= g_\alpha^2 g_\beta^2 \int \frac{d^3k}{(2\pi)^3} \int \frac{dk^0}{2\pi} 2 \operatorname{Im}[V_{\alpha\beta}(k^0, \vec{k}, q^0, \vec{q})] \mathcal{P} \left[-\frac{1}{(k^0)^2} \right] \\ &\quad \times C_{AB}^\alpha C_{CD}^\beta \Gamma_{\alpha(1)}^A(\vec{k}) \Gamma_{\beta(1)}^C(-[\vec{k}+\vec{q}]) \Gamma_{\alpha(2)}^B(-\vec{k}) \Gamma_{\beta(2)}^D(\vec{k}+\vec{q}) \left[1 + \mathcal{O}\left(\frac{1}{N_c}\right) \right]. \end{aligned} \quad (25)$$

Similarly, the crossed-box contribution coming entirely from the meson singularities is

$$\begin{aligned} \mathcal{M}_X &= g_\alpha^2 g_\beta^2 \int \frac{d^3k}{(2\pi)^3} \int \frac{dk^0}{2\pi} 2 \operatorname{Im}[V_{\alpha\beta}(k^0, \vec{k}, q^0, \vec{q})] C_{AB}^\alpha C_{CD}^\beta \Gamma_{\alpha(1)}^A(\vec{k}) \Gamma_{\beta(1)}^C(-[\vec{k}+\vec{q}]) \Gamma_{\beta(2)}^D(\vec{k}+\vec{q}) \Gamma_{\alpha(2)}^B(-\vec{k}) \\ &\quad \times \mathcal{P} \left[\frac{1}{(k^0 + q^0 + |\vec{p}|^2/2m_B - |\vec{p}+\vec{k}+\vec{q}|^2/2m_B)(k^0 + |\vec{p}|^2/2m_B - |\vec{p}-\vec{k}|^2/2m_B)} \right] \\ &= g_\alpha^2 g_\beta^2 \int \frac{d^3k}{(2\pi)^3} \int \frac{dk^0}{2\pi} 2 \operatorname{Im}[V_{\alpha\beta}(k^0, \vec{k}, q^0, \vec{q})] \mathcal{P} \left[\frac{1}{(k^0)^2} \right] \\ &\quad \times C_{AB}^\alpha C_{CD}^\beta \Gamma_{\alpha(1)}^A(\vec{k}) \Gamma_{\beta(1)}^C(-[\vec{k}+\vec{q}]) \Gamma_{\beta(2)}^D(\vec{k}+\vec{q}) \Gamma_{\alpha(2)}^B(-\vec{k}) \left[1 + \mathcal{O}\left(\frac{1}{N_c}\right) \right]. \end{aligned} \quad (26)$$

Note that only in the nonrelativistic limit the principal values of the baryon propagators are equal and opposite for both $\mathcal{M}_\square^{ret}$ and \mathcal{M}_X . As a result, the sum of these two contributions is proportional to a spin-flavor commutator,

$$\begin{aligned} \mathcal{M}_\square^{ret} + \mathcal{M}_X &= g_\alpha^2 g_\beta^2 \int \frac{d^3k}{(2\pi)^3} \int \frac{dk^0}{2\pi} 2 \operatorname{Im}[V_{\alpha\beta}(k^0, \vec{k}, q^0, \vec{q})] \mathcal{P} \left[-\frac{1}{(k^0)^2} \right] C_{AB}^\alpha C_{CD}^\beta \Gamma_{\alpha(1)}^A(\vec{k}) \Gamma_{\beta(1)}^C(-\vec{k}-\vec{q}) \\ &\quad \times [\Gamma_{\alpha(2)}^B(-\vec{k}), \Gamma_{\beta(2)}^D(\vec{k}+\vec{q})] \left[1 + \mathcal{O}\left(\frac{1}{N_c}\right) \right]. \end{aligned} \quad (27)$$

In general, we have to include both orderings of the exchanged mesons. In Eq. (27) the first meson is α . Changing the meson sequence and keeping the loop momenta flow unchanged we get

$$\begin{aligned}
\mathcal{M}_{\square}^{ret} + \mathcal{M}_X &= g_\alpha^2 g_\beta^2 \int \frac{d^3 k}{(2\pi)^3} \int \frac{dk^0}{2\pi} 2 \text{Im}[V_{\alpha\beta}(k^0, \vec{k}, q^0, \vec{q})] \\
&\times \text{P} \left[-\frac{1}{(k^0)^2} \right] C_{AB}^\alpha C_{CD}^\beta \\
&\times [\Gamma_{\beta(1)}^C(\vec{k}), \Gamma_{\alpha(1)}^A(-\vec{k}-\vec{q})] \\
&\times \Gamma_{\beta(2)}^D(-\vec{k}) \Gamma_{\alpha(2)}^B(\vec{k}+\vec{q}) \left[1 + O\left(\frac{1}{N_c}\right) \right], \quad (28)
\end{aligned}$$

where we used $V_{\beta\alpha} = V_{\alpha\beta}$. Now, the commutator involves the meson couplings along a different baryon line.

The large- N_c scaling of the retardation effect and the crossed-box diagram taken separately is given by the product of the coupling constants $g_\alpha^2 g_\beta^2$. However, as seen from Eqs. (27) and (28), their total contribution is proportional to the commutators of the spin-flavor operators evaluated between the ground state baryons. The cancellation between the retardation effect and the crossed-box contribution up to higher-order corrections happens due to the presence of the commutator.

A number of mesons shown in Tables I and II make identical contributions to the spin-flavor structure of the nucleon-nucleon potential, Eq. (6). For example, f_0 and the time component of the ω contribute to the isoscalar central potential V_0^0 ; the π and spatial components of ρ contribute to the isovector tensor force. Other such pairs are a_0 and ρ^i , η and $\bar{\omega}$, π and $\bar{\rho}$. Thus, out of ten couplings in Tables I and II there are only six independent structures. They give 36 different combinations for two-meson exchange graphs counting combinations differing in the meson sequence. Out of this the number of distinct meson pairs is 21.

The commutators in Eqs. (27) and (28) vanish identically for those graphs in which at least one of the mesons is f_0 (or ω^i). The reason is that the spin-flavor structure of f_0 (ω^i) is given by the unity operator, which commutes with any other operator. This insures the large N_c consistency of the two-meson box and crossed-box diagrams containing the following six (independent) pairs of mesons:

$$(f_0 f_0), (f_0 \vec{f}_1), (f_0 \eta), (f_0 a_0), (f_0 \vec{a}_1), (f_0 \pi). \quad (29)$$

Note, as discussed above, the same cancellation occurs when ω^i is exchanged instead of f_0 .

Similar cancellations occur for contributions of the box and crossed-box diagrams containing the following pairs of mesons:

$$(a_0 \eta), (a_0 \vec{f}_1), \quad (30)$$

since the spin-flavor structure of a_0 couplings contains only I^a generators while the couplings of \vec{f}_1 and η contain only J^i generators, which commute with I^a , Eq. (1).

A number of the meson-baryon couplings in Tables I and II are of order $N_c^{-1/2}$. Hence, the exchange of any pair of such mesons is suppressed by at least N_c^{-2} and, therefore,

cannot violate the KSM counting rules. These are the exchanges of the following meson pairs:

$$(a_0 a_0), (\eta \eta), (\vec{f}_1 \vec{f}_1), (\eta \vec{f}_1), [(a_0 \eta), (a_0 \vec{f}_1)], \quad (31)$$

where the meson pairs in the square brackets have been previously considered, Eq. (30).

This leaves us with nine nontrivial meson pair exchanges whose contributions via the box and crossed-box diagrams can potentially spoil the KSM counting rules. Out of these, three pairs couple to baryons only via nonderivative couplings,

$$\begin{aligned}
(a_0 \vec{a}_1), (\vec{f}_1 \vec{a}_1), &\rightarrow O(N_c^0), \\
(\vec{a}_1 \vec{a}_1), &\rightarrow O(N_c^2), \quad (32)
\end{aligned}$$

and the remaining six pairs require one or two derivative couplings,

$$\begin{aligned}
(a_0 \pi), (\eta \pi), (\eta \vec{a}_1), (\pi \vec{f}_1), &\rightarrow O(N_c^0), \\
(\pi \pi), (\pi \vec{a}_1), &\rightarrow O(N_c^2). \quad (33)
\end{aligned}$$

In Eqs. (32) and (33) the large- N_c scaling of the product of corresponding coupling constants $g_\alpha^2 g_\beta^2$ in the box and the crossed-box diagrams has also been indicated.

The considerations of the meson pairs in Eq. (32) are simpler than those with derivatively coupled mesons, Eq. (33), and will be considered first. The analysis of the exchanges with derivative couplings requires performing angular integration and is done in the Appendix.

The retardation effect, Eq. (25), and the crossed-box diagram, Eq. (26), involving exchanges of a_0 and \vec{a}_1 contribute to isoscalar and isovector spin-spin, V_σ^0 and V_σ^1 , terms; the (\vec{f}_1, \vec{a}_1) exchange contains a V_σ^1 term in addition to V_σ^1 . The N_c^0 -order contributions to V_σ^0 and V_σ^0 from (a_0, \vec{a}_1) and (\vec{f}_1, \vec{a}_1) exchanges violate the KSM rules, Eq. (8). Fortunately, these contributions are canceled in the sum of the retardation effect and crossed-box diagram, Eqs. (27) and (28),

$$\begin{aligned}
&C_{AB}^{\vec{f}_1} C_{CD}^{\vec{a}_1} \Gamma_{\vec{f}_1(1)}^A(\vec{k}) \Gamma_{\vec{a}_1(1)}^C(-[\vec{k}+\vec{q}]) \\
&\times [\Gamma_{\vec{f}_1(2)}^B(-\vec{k}), \Gamma_{\vec{a}_1(2)}^D(\vec{k}+\vec{q})] \\
&= J_{(1)}^i X_{(1)}^{ja} [J_{(2)}^i, X_{(2)}^{ja}] \\
&= \frac{1}{2} (\{J_{(1)}^i, X_{(1)}^{ja}\} + [J_{(1)}^i, X_{(1)}^{ja}]) [J_{(2)}^i, X_{(2)}^{ja}] \\
&= 2 X_{(1)}^{ka} X_{(2)}^{ka} + O\left(\frac{1}{N_c^2}\right), \quad (34)
\end{aligned}$$

for (\vec{f}_1, \vec{a}_1) exchange and similarly for (a_0, \vec{a}_1) exchange. In the last step in Eq. (34) we used the commutation and anti-commutation relations of the generators of the contracted

SU(4) symmetry, Eqs. (1) and (5). Thus, these exchanges, when both box and crossed-box diagrams are included, contribute only to the isovector spin-spin term of the nucleon-nucleon potential up to corrections of order N_c^{-2} . This is an allowable contribution by KSM counting rules.

The box and crossed-box diagrams corresponding to (\vec{a}_1, \vec{a}_1) exchange are of order N_c^2 . The corresponding retardation effect and crossed-box diagram separately contribute to V_0^0 , V_σ^0 , and V_σ^0 . The first two terms are of order N_c and the third term is of order N_c^{-1} , Eq. (8). However, the product of the spin-flavor structures in Eqs. (27) and (28) is of order N_c^{-4} ,

$$\begin{aligned} & C_{AB}^{a_1} C_{CD}^{a_1} \Gamma_{a_1(1)}^A(\vec{k}) \Gamma_{a_1(1)}^C(-[\vec{k} + \vec{q}]) \\ & \times [\Gamma_{a_1(2)}^B(-\vec{k}), \Gamma_{a_1(2)}^D(\vec{k} + \vec{q})] \\ & = X_{(1)}^{ia} X_{(1)}^{jb} [X_{(2)}^{ia}, X_{(2)}^{jb}] \\ & = \frac{1}{2} (\{X_{(1)}^{ia}, X_{(1)}^{jb}\} + [X_{(1)}^{ia}, X_{(1)}^{jb}]) [X_{(2)}^{ia}, X_{(2)}^{jb}] \\ & = \frac{1}{2} [X_{(1)}^{ia}, X_{(1)}^{jb}] [X_{(2)}^{ia}, X_{(2)}^{jb}] \sim O\left(\frac{1}{N_c^4}\right), \end{aligned} \quad (35)$$

where in the third step we used the fact that the anticommutator is symmetric and the commutator is antisymmetric under the simultaneous exchange of the spin-flavor indices $(ia) \rightarrow (jb)$; the large N_c of the baryon matrix elements of $[X^{ia}, X^{jb}]$ is given in Eq. (2). Combining the N_c^4 suppression in Eq. (35) with the N_c^2 scaling of the product $g_{a_1}^4$ we see that the sum in Eq. (27) [and similarly in Eq. (28)] is of order N_c^{-2} , which is consistent with KSM counting rules. Note that in this case full contracted SU(4) algebra has to be used to ensure the cancellation. Thus, the cancellation of the retardation effect against the crossed-box diagram requires an inclusion of both nucleon and Δ intermediate states. If one restricts the intermediate states to nucleons only, the cancellation would not occur.

Thus far, we have shown that the retardation effect of all two-meson exchange diagrams without derivative couplings, Eq. (32), cancel against the corresponding crossed-box graphs. As is shown in the Appendix, similar cancellations occur for the remaining six meson pairs, Eq. (33), which involve one or two derivatively coupled mesons.

In addition to box and crossed-box diagrams, any pair of mesons can be exchanged via triangle (or ‘‘seagull’’) diagrams, Fig. 5, containing a four-point meson-baryon vertex. The spin-flavor structure of this vertex is given by the product of two $\Gamma_{\alpha(n)}^A(\vec{k})$ operators. The four-point meson-baryon coupling is of order N_c^0 for any meson pair [2]. Hence, the largest scaling of a triangle diagram is N_c , e.g., when two pions or f_0 and ω' are exchanged. Thus, the triangle graph cannot violate the scaling of the leading $O(N_c)$ spin-flavor terms, Eq. (8). However, the subleading $O(N_c^{-1})$ terms might be sensitive to contributions from the triangle dia-

grams. Since these diagrams contain only one baryon propagator, its pole does not contribute to the potential (the contour of the complex k^0 integration can always be closed in such a way as to avoid the baryon pole). As we will show shortly, the contributions from the meson singularities in the triangle graphs add up to cancel all terms that violate the KSM counting rules.

A given triangle graph can be associated with a corresponding box or crossed-box diagram by shrinking the appropriate baryon propagator to zero. It can then be shown that the sum of the appropriate pair of the triangle graphs, shown in Fig. 5, is similar to Eqs. (27) or (28). The essential point in the above discussion was the presence of the commutator in Eqs. (27) and (28). The same commutator appears in the sum of the triangle graphs.

What are the pairs of the triangle graphs that correspond to the box and crossed-box diagrams, which led to Eqs. (27) and (28)? These graphs contain the same meson pairs. The two corresponding graphs differ according to which baryon line the four-point meson-baryon vertex is attached to Fig. 5. In addition, two Γ structures at the four-point vertex of one of the corresponding graphs are in opposite order relative to the sequence of these structures in the other graph. This leads to the appearance of a commutator in the sum of the corresponding triangle graphs.

In the case of the box and crossed-box diagrams the direction of the energy flow assured that the retardation effect and the crossed-box contribution are equal and opposite up to $1/N_c$ corrections. The sign difference was due to the product of the principle values of the baryon propagators (after the nonrelativistic reduction), Eqs. (25) and (26), which had different signs for the box and crossed-box diagrams. Despite the presence of only a single baryon propagator, the contributions from each of the corresponding triangle graphs come with opposite signs due to the different flow of the energy and momenta, Fig. 5. The sum of these two graphs is

$$\begin{aligned} \mathcal{M}_1 + \mathcal{M}_2 &= g_{\alpha\beta} g_{\beta\gamma} g_{\alpha\beta} \int \frac{d^3k}{(2\pi)^3} \int \frac{dk^0}{2\pi} 2 \text{Im}[V_{\alpha\beta}(k^0, \vec{k}, q^0, \vec{q})] \\ & \times \text{P}\left[-\frac{1}{k^0}\right] C_{AB}^\alpha C_{CD}^\beta \Gamma_{\alpha(1)}^A(\vec{k}) \Gamma_{\beta(1)}^C(-\vec{k} - \vec{q}) \\ & \times [\Gamma_{\alpha(2)}^B(-\vec{k}), \Gamma_{\beta(2)}^D(\vec{k} + \vec{q})] \left[1 + O\left(\frac{1}{N_c}\right)\right], \end{aligned} \quad (36)$$

where $g_{\alpha\beta}$ (order N_c^0 for all α and β) is the coupling constant of the four-point vertex and the function $V_{\alpha\beta}$ is given by Eq. (21) provided $\tilde{V}_{\alpha\beta}$ contains the product of the three meson-baryon vertex functions (including one corresponding to the four-point vertex). A similar expression can be written for the sum of the two triangle graphs in which the sequence of the α and β mesons is changed as in Eq. (28).

It is clear that the sum in Eq. (36) contributes to the same spin-flavor terms as the sum in Eq. (27): both expressions contain identical spin-flavor structures. The differences in the integrands are irrelevant as far as the cancellations in Eqs.

(27) and (28) are concerned. As a result, the large- N_c scaling of the contribution in Eq. (36) is that of Eq. (27) times scaling of $(g_\alpha g_\beta)^{-1}$.

Hence, when all the contributions of the triangle graphs are included, the resulting spin-flavor terms are consistent with the KSM counting rules, Eq. (8).

IV. CONCLUSION

At a technical level we have shown by explicit calculation that if meson-baryon couplings scale according to the standard large- N_c rules, then the two-meson-exchange contributions to the nonrelativistic baryon-baryon potential are consistent with the large- N_c KSM scaling rules deduced in Refs. [6,7]. This is highly nontrivial since the derivation of these rules in Refs. [6,7] only included diagrams that correspond to one-meson exchange when translated to the hadronic level. This certainly adds confidence that Refs. [6,7] correctly described the N_c scaling behavior of the nucleon-nucleon potential in the large- N_c limit of QCD. The essential issue in the calculations here was that the retardation contributions to the potential from the box graph cancel against the crossed-box contributions for all spin-isospin structures in the potential where the retardation contributions or the crossed-box contributions separately violate the counting rules.

The derivation presented here was done in a “brute force” manner. Namely, we considered the various meson exchanges one at a time, identified the contributions to the various spin-isospin structures that apparently violated the KSM large- N_c scalings, and showed that in all cases they canceled. It would be very useful to find a more general method for demonstrating the cancellation. While the methods used here were adequate for the two-meson-exchange case, it would be extremely cumbersome to extend them to three-meson exchange or higher. Given the cancellations for all “dangerous” contributions at the two-meson-exchange level it seems reasonable to expect that such cancellations will occur for any number of meson exchanges and that the full baryon-baryon potential will be consistent with the KSM scaling rules. However, a general proof of the cancellations for all orders would be desirable.

In the Introduction it was argued that the large- N_c scaling behavior of the baryon-baryon interactions gives some general insights into the underlying physics arising from QCD. In particular, it was argued that a consistent picture emerged and five aspects of this picture were enumerated. Let us now briefly discuss how the calculations discussed above support this picture.

The first point raised was that while a nonrelativistic potential used to describe the interaction has overall strength of order N_c , the kernel of a Bethe-Salpeter equation does not have a simple N_c dependence. As noted many times, the N_c^2 -order contribution to the potential from the crossed-box graph is canceled by the retardation effect from the box graph. However, such a cancellation cannot happen in the context of the Bethe-Salpeter equation. The entire box graph (including meson pole contributions) is an iterate of the Bethe-Salpeter kernel and hence cannot be included as a contribution to the kernel. Thus, in the Bethe-Salpeter context

there is no part of the box graph to cancel the N_c^2 -order contribution from the crossed box. Therefore, unlike the potential, the Bethe-Salpeter kernel cannot be associated with an overall strength of N_c . Presumably, the Bethe-Salpeter kernel has contributions scaling as N_c to all powers arising from multiple meson exchanges.

The second point made was that the meson-exchange picture of baryon-baryon interactions with the leading part of the potential scaling as N_c is consistent with the meson-exchange picture of the potential provided the momentum exchanged is of order N_c^0 . It was shown explicitly using nonrelativistic kinematics that at the level of two-meson exchange, all “dangerous” contributions to the potential canceled so that there is no inconsistency with a potential scaling as N_c . It is reasonable to expect the behavior to hold for any number of meson exchanges. If true, this strengthens the case for using meson-exchange models to describe nucleon-nucleon interactions.

However, it was also argued that the idea of a potential described by the meson-exchange picture is unsuitable for momenta of order N_c . At a technical level this is apparent in Eqs. (17), (18), (24), and (25) where the cancellations of the box and crossed-box graphs depend explicitly on the nonrelativistic form of the propagator. If momenta of order N_c were used, the cancellations clearly fail to occur. Thus the usefulness of the meson-exchange picture is not evident for momenta of order N_c . In fact, it is quite satisfying that the evidence of consistency breaks down in this regime for a number of reasons. In the first place Witten’s TDH picture of baryon-baryon interactions is more appropriate for $p \sim N_c$. This picture has no obvious meson-exchange interpretation. The internal structure of each baryon is distorted in the presence of the other. Moreover, it is not surprising from a more traditional hadronic viewpoint that a meson-exchange potential picture breaks down in this regime. If $p \sim N_c$ and $m_N \sim N_c$ then the kinetic energy of the baryons is also of order N_c . Since meson masses are of order N_c^0 , an increasing number of mesons are produced. It is hardly surprising that the potential picture breaks down in this situation.

A fourth point raised in the Introduction was that relative sizes of the various spin-isospin structures in the nucleon-nucleon potential are consistent at the two-meson-exchange level with those deduced from the contracted SU(4) structure of KSM. Moreover, if one looks carefully at all of the cancellations, one finds that corrections to the leading behavior were all $1/N_c^2$ suppressed. This is consistent with Refs. [6,7] where it is found that subleading spin-isospin structures are down by factors $1/N_c^2$. Overall this strongly supports the view that the expansion is in fact in $1/N_c^2$ rather than in $1/N_c$.

The final point stressed was that the Δ plays an essential role. As is evident from Eqs. (35) and the Appendix, the cancellations between the box and crossed-box graphs do not occur if intermediate states are restricted entirely to nucleons; Δ resonances are required as intermediate states. More generally one expects that as the contracted SU(4) structure is used to obtain cancellations, the entire $I=J=1/2, 3/2, 5/2, \dots$ tower of baryon states can contribute. Up to two-meson exchange with nucleon as initial and final

states, however, only nucleons and Δ 's can contribute.

The formal consistency of the large- N_c treatment and the meson-exchange picture is quite satisfying. However, considerable caution should be exercised in trying to draw conclusions about the real world of $N_c = 3$. We have used $1/N_c$ as a counting parameter to distinguish large from small contributions. This is clearly legitimate if all the coefficients multiplying these factors are natural, i.e., of order unity. However, all coefficients are not natural. One key difficulty is that the meson-exchange picture is being used here to connect hadronic phenomena with nuclear phenomena. However, the scales in nuclear physics are generally much smaller than those in hadronic physics [5]. It is not clear directly from QCD why these nuclear scales are so small and it is generally thought to be "accidental." The interplay between small nuclear scales (that may be large in a $1/N_c$ sense) with much larger hadronic scales (that may be small formally in a $1/N_c$ sense) can potentially spoil the results of a straightforward $1/N_c$ approach. To show how extreme this problem may be we can consider the deuteron binding energy B (which is formally of order N_c) and the Δ -nucleon mass difference $m_\Delta - m_N$ (which is order $1/N_c$). If all coefficients were natural, one would expect B to be an order of magnitude larger than $m_\Delta - m_N$, whereas, in fact, it is two orders of magnitude smaller. It would not be surprising that difficulties might arise when calculating B if one neglects $m_\Delta - m_N$ as being "small."

The large- N_c structure of the nucleon-nucleon potential has been so far used phenomenologically in two contexts. The first is as an attempt to justify the observed approximate Wigner SU(4) symmetry [12] in light nuclei as arising from the underlying contracted SU(4) structure in the large- N_c potential [6]. The second is an attempt to justify the qualitative sizes of the spin-flavor structures in phenomenological potentials as being explained by the contracted SU(4) structure in the large- N_c potential [6,7]. It is not immediately obvious that these two explanations are legitimate in light of qualitatively distinct nuclear scales that are not associated with the $1/N_c$ expansion. Clearly, this issue needs further investigation. However, it is also not immediately clear how to formulate a systematic expansion, which incorporates the $1/N_c$ scaling rules while allowing nuclear scales to be much smaller [13] than hadronic scales. The comparison of the qualitative sizes of the spin-flavor structures in phenomenological potentials with what is expected from large N_c raises another issue. The potentials predicted in large N_c are not nucleon-nucleon potentials; rather, they are coupled channel potentials for the full tower of $I=J$ baryon states including an explicit Δ . The phenomenological potentials to which they are compared have the explicit Δ 's integrated out. It is by no means clear that the act of integrating out Δ 's does not alter the spin-flavor structure. Again, this requires further study.

Given these possible difficulties in drawing phenomenological conclusions from large- N_c potentials, one might ask about the relevance for the real world of our demonstration that large- N_c counting rules are consistent with the meson-exchange picture of potentials at the two-meson-exchange level. Of course, it remains possible that after a careful study

one may find that the particular phenomenological predictions to date—the Wigner SU(4) symmetry and the characteristic relative sizes of the various terms in phenomenological potentials—are robust and remain valid even after the smallness of the typical nuclear scales are included. Whether or not this turns out to be the case, however, we may still be able to learn qualitatively interesting things. For example, the cancellations seen in the two-pion-exchange graphs require that Δ intermediate states be included. For $N_c = 3$, one does not expect such cancellations to be perfect, but the general tendency to cancel should survive. This suggests that Δ box and crossed-box contributions should be comparable in size to those with nucleon intermediate states. This issue may be relevant for potential models motivated by chiral symmetry where two-pion-exchange contributions with nucleon intermediate states are included at next-to-leading order but explicit Δ contributions are not included [13]. At a more qualitative level, the fact that at large N_c a meson-exchange motivated picture of the potential is consistent gives at least some support for the view that more generally nucleon-nucleon interactions can be described in terms of meson exchanges.

ACKNOWLEDGMENTS

This work was supported by the U.S. Department of Energy, Grant No. DE-FG02-93ER-40762. T.D.C. wishes to acknowledge discussions with M. Luty, D. Phillips, J. Friar, F. Gross, and S. Wallace. He also acknowledges support at the INT where progress was made on this work.

APPENDIX

In this appendix we discuss the box and crossed-box graphs with one or two derivative couplings, Eq. (33). As in the case of the nonderivatively coupled mesons, Eq. (32), the sum of the retardation effect and the crossed-box diagram can be written as the sum of the products of anticommutators and commutators of the spin-flavor generators. The cancellation of the terms that violated spin-flavor counting rules essentially has occurred due the symmetry properties of these products under the interchange of the spin-flavor symmetry. The remaining terms are either consistent with the counting rules or suppressed by $1/N_c^2$ as in Eq. (35). However, when derivatively coupled mesons are included, the symmetry of the products of commutators and anticommutators under the interchange of spin-flavor symmetry is broken due to the contraction of the spin-flavor generators with momentum indices. In order to see the cancellation, the angular integration in Eqs. (27) and (28) must be performed. In this appendix the cancellation is shown for the two-pion-exchange diagrams. The exchanges involving other pairs of mesons, Eq. (33), are essentially identical to this case.

The retardation effect and the crossed-box contribution is given in Eq. (27), which has the following form for the two-pion exchange:

$$\begin{aligned}
\mathcal{M}_{\square}^{ret} + \mathcal{M}_X &= g_{\pi}^4 \int \frac{d^3 k}{(2\pi)^3} \int \frac{dk^0}{2\pi} \mathcal{P} \left[-\frac{1}{(k^0)^2} \right] \\
&\quad \times 2 \operatorname{Im} [V_{\pi\pi}(k^0, \vec{k}, q^0, \vec{q})] \\
&\quad \times X_{(1)}^{ia} X_{(1)}^{jb} [X_{(2)}^{la}, X_{(2)}^{rb}] \vec{k}^i \vec{k}^l (\vec{k}^j + \vec{q}^j) (\vec{k}^r + \vec{q}^r) \\
&\quad \times \left[1 + \mathcal{O}\left(\frac{1}{N_c}\right) \right]. \tag{A1}
\end{aligned}$$

After k^0 integration Eq. (A1) reduces to

$$\begin{aligned}
\mathcal{M}_{\square}^{ret} + \mathcal{M}_X &= g_{\pi}^4 \int \frac{k^2 dk}{(2\pi)^3} \int d\Omega F(|\vec{k}|, |\vec{q}|, \vec{k} \cdot \vec{q}, q^0) \\
&\quad \times X_{(1)}^{ia} X_{(1)}^{jb} [X_{(2)}^{la}, X_{(2)}^{rb}] \vec{k}^i \vec{k}^l (\vec{k}^j + \vec{q}^j) (\vec{k}^r + \vec{q}^r), \tag{A2}
\end{aligned}$$

where the explicit form of the function $F(|\vec{k}|, |\vec{q}|, \vec{k} \cdot \vec{q}, q^0)$ is not required for the following discussion.

Let us consider the angular integration in Eq. (A2),

$$I_{\Omega} \equiv \int d\Omega F(|\vec{k}|, |\vec{q}|, \vec{k} \cdot \vec{q}, q^0) \vec{k}^i \vec{k}^l (\vec{k}^j + \vec{q}^j) (\vec{k}^r + \vec{q}^r). \tag{A3}$$

The general form of this integral is

$$\begin{aligned}
I_{\Omega} &= (\delta^{ij} \delta^{lr} + \delta^{il} \delta^{jr} + \delta^{ir} \delta^{jl}) f_1(|\vec{k}|, |\vec{q}|, q^0) \\
&\quad + q^i q^j q^l q^r f_2(|\vec{k}|, |\vec{q}|, q^0) \\
&\quad + (\delta^{il} q^j q^r + \delta^{lr} q^i q^l) f_3(|\vec{k}|, |\vec{q}|, q^0) \\
&\quad + (\delta^{ij} q^l q^r + \delta^{lr} q^j q^l + \delta^{il} q^i q^r) \\
&\quad + \delta^{lr} q^i q^j f_4(|\vec{k}|, |\vec{q}|, q^0), \tag{A4}
\end{aligned}$$

where functions f_1 , f_2 , f_3 , and f_4 do not depend on $\vec{k} \cdot \vec{q}$. The form of the I_{Ω} can be obtained from general arguments based on the symmetry properties of Eq. (A3) under the various exchanges of the momentum indices.

Each term in Eq. (A4) when combined with spin-flavor generators in Eq. (A1) is suppressed by N_c^{-4} . Let us see how it comes about for each term separately.

The first product of Kronecker deltas in the f_1 term leads to

$$\begin{aligned}
&\delta^{ij} \delta^{lr} X_{(1)}^{ia} X_{(1)}^{jb} [X_{(2)}^{la}, X_{(2)}^{rb}] \\
&= X_{(1)}^{ia} X_{(1)}^{ib} [X_{(2)}^{la}, X_{(2)}^{lb}] \\
&= \frac{1}{2} (\{X_{(1)}^{ia}, X_{(1)}^{ib}\} + [X_{(1)}^{ia}, X_{(1)}^{ib}]) [X_{(2)}^{la}, X_{(2)}^{lb}] \\
&= \frac{1}{2} \{X_{(1)}^{ia}, X_{(1)}^{ib}\} [X_{(2)}^{la}, X_{(2)}^{lb}] + \frac{1}{2} [X_{(1)}^{ia}, X_{(1)}^{ib}] [X_{(2)}^{la}, X_{(2)}^{lb}] \\
&= \mathcal{O}\left(\frac{1}{N_c^4}\right), \tag{A5}
\end{aligned}$$

where the product of the commutator and the anticommutator vanishes because the commutator is antisymmetric under the $a \leftrightarrow b$ exchange while the anticommutator is symmetric. The remaining product of the two commutators is of order N_c^{-4} from Eq. (3). Thus, an overall contribution of this term is of order N_c^{-2} , which is consistent with KSM counting rules, Eq. (8). Note how the angular averaging of Eq. (A3) induced symmetry properties of the spin-flavor matrices in Eq. (A1).

The second product of Δ 's in f_1 leads to an expression identical to Eq. (35); its contribution, therefore, is suppressed by N_c^{-4} as well. The suppression of the last term multiplying the f_1 is easily observed,

$$\begin{aligned}
&\delta^{ir} \delta^{jl} X_{(1)}^{ia} X_{(1)}^{jb} [X_{(2)}^{la}, X_{(2)}^{rb}] \\
&= X_{(1)}^{ia} X_{(1)}^{ib} [X_{(2)}^{ja}, X_{(2)}^{ib}] \\
&= \frac{1}{2} (\{X_{(1)}^{ia}, X_{(1)}^{ib}\} + [X_{(1)}^{ia}, X_{(1)}^{ib}]) [X_{(2)}^{ja}, X_{(2)}^{ib}] \\
&= \frac{1}{2} \{X_{(1)}^{ia}, X_{(1)}^{ib}\} [X_{(2)}^{ja}, X_{(2)}^{ib}] + \mathcal{O}\left(\frac{1}{N_c^4}\right) = \mathcal{O}\left(\frac{1}{N_c^4}\right), \tag{A6}
\end{aligned}$$

where in the last step we used antisymmetry under the simultaneous exchanges $a \leftrightarrow b$ and $i \leftrightarrow j$,

$$\{X_{(1)}^{ia}, X_{(1)}^{jb}\} [X_{(2)}^{ja}, X_{(2)}^{ib}] = -\{X_{(1)}^{ia}, X_{(1)}^{ib}\} [X_{(2)}^{ja}, X_{(2)}^{ib}]. \tag{A7}$$

Similarly, the product of the four components of the external momenta multiplying f_2 is of order N_c^{-4} ,

$$\begin{aligned}
&q^i q^j q^l q^r X_{(1)}^{ia} X_{(1)}^{jb} [X_{(2)}^{la}, X_{(2)}^{rb}] \\
&= \frac{1}{2} q^i q^j q^l q^r \{X_{(1)}^{ia}, X_{(1)}^{jb}\} [X_{(2)}^{la}, X_{(2)}^{rb}] + \mathcal{O}\left(\frac{1}{N_c^4}\right) \\
&= \mathcal{O}\left(\frac{1}{N_c^4}\right), \tag{A8}
\end{aligned}$$

where the vanishing of the last product can be seen after the substitution $a \leftrightarrow b$, $i \leftrightarrow j$, and $l \leftrightarrow r$,

$$\begin{aligned}
&q^i q^j q^l q^r \{X_{(1)}^{ia}, X_{(1)}^{jb}\} [X_{(2)}^{la}, X_{(2)}^{rb}] \\
&= -q^i q^j q^l q^r \{X_{(1)}^{ia}, X_{(1)}^{jb}\} [X_{(2)}^{la}, X_{(2)}^{rb}]. \tag{A9}
\end{aligned}$$

Similar arguments can be used to show the vanishing [up to $\mathcal{O}(N_c^{-4})$] of the term containing the function f_3 :

$$\begin{aligned}
 & (\delta^{il} q^j q^r + \delta^{jr} q^i q^l) X_{(1)}^{ia} X_{(1)}^{jb} [X_{(2)}^{la}, X_{(2)}^{rb}] \\
 &= q^j q^r X_{(1)}^{ia} X_{(1)}^{jb} [X_{(2)}^{ia}, X_{(2)}^{rb}] + q^i q^l X_{(1)}^{ia} X_{(1)}^{jb} [X_{(2)}^{la}, X_{(2)}^{jb}] \\
 &= q^j q^l X_{(1)}^{ia} X_{(1)}^{jb} [X_{(2)}^{ia}, X_{(2)}^{lb}] + q^j q^l X_{(1)}^{ja} X_{(1)}^{ib} [X_{(2)}^{la}, X_{(2)}^{ib}] \\
 &= q^j q^l X_{(1)}^{ia} X_{(1)}^{jb} [X_{(2)}^{ia}, X_{(2)}^{lb}] + q^j q^l X_{(1)}^{jb} X_{(1)}^{ia} [X_{(2)}^{ia}, X_{(2)}^{lb}] \\
 &= q^j q^l [X_{(1)}^{ia}, X_{(1)}^{jb}] [X_{(2)}^{ia}, X_{(2)}^{lb}] = O\left(\frac{1}{N_c^4}\right), \quad (\text{A10})
 \end{aligned}$$

where in the second equality we changed the index r into l in the first term and exchanged $i \leftrightarrow j$ in the second term; in the next step we make the $a \leftrightarrow b$ exchange in the second term.

The first term multiplying f_4 in Eq. (A4) is suppressed as follows:

$$\begin{aligned}
 & \delta^{ij} q^l q^r X_{(1)}^{ia} X_{(1)}^{jb} [X_{(2)}^{la}, X_{(2)}^{rb}] \\
 &= q^l q^r X_{(1)}^{ia} X_{(1)}^{ib} [X_{(2)}^{la}, X_{(2)}^{rb}] \\
 &= \frac{1}{2} q^l q^r \{X_{(1)}^{ia}, X_{(1)}^{ib}\} [X_{(2)}^{la}, X_{(2)}^{rb}] + O\left(\frac{1}{N_c^4}\right) \\
 &= O\left(\frac{1}{N_c^4}\right) \quad (\text{A11})
 \end{aligned}$$

where the vanishing of the last product can be seen via the substitution $a \leftrightarrow b$ followed by $l \leftrightarrow r$. Similar arguments apply for the last term multiplying f_4 .

Lastly, the sum of the remaining two terms in Eq. (A4) multiplying f_4 vanishes [up to $O(N_c^{-4})$] as follows:

$$\begin{aligned}
 & (\delta^{ir} q^j q^l + \delta^{jl} q^i q^r) X_{(1)}^{ia} X_{(1)}^{jb} [X_{(2)}^{la}, X_{(2)}^{rb}] \\
 &= q^j q^l X_{(1)}^{ia} X_{(1)}^{jb} [X_{(2)}^{la}, X_{(2)}^{ib}] + q^i q^r X_{(1)}^{ia} X_{(1)}^{jb} [X_{(2)}^{ja}, X_{(2)}^{rb}] \\
 &= q^i q^l X_{(1)}^{ja} X_{(1)}^{ib} [X_{(2)}^{la}, X_{(2)}^{jb}] + q^i q^l X_{(1)}^{ia} X_{(1)}^{jb} [X_{(2)}^{ja}, X_{(2)}^{lb}] \\
 &= q^i q^l X_{(1)}^{ja} X_{(1)}^{ib} [X_{(2)}^{la}, X_{(2)}^{jb}] + q^i q^l X_{(1)}^{ib} X_{(1)}^{ja} [X_{(2)}^{jb}, X_{(2)}^{la}] \\
 &= \frac{1}{2} q^i q^l \{X_{(1)}^{ja}, X_{(1)}^{ib}\} [X_{(2)}^{la}, X_{(2)}^{jb}] + \frac{1}{2} q^i q^l \{X_{(1)}^{ib}, X_{(1)}^{ja}\} \\
 &\quad \times [X_{(2)}^{jb}, X_{(2)}^{la}] + O\left(\frac{1}{N_c^4}\right) \\
 &= O\left(\frac{1}{N_c^4}\right), \quad (\text{A12})
 \end{aligned}$$

where in the second equality we changed $i \leftrightarrow ji$ and $r \leftrightarrow l$ in the first and second term respectively; in the next step the change is $a \leftrightarrow b$ in the second term.

This completes the discussion of two-pion exchange box and crossed-box diagrams. Their mutual contribution has an overall scaling of N_c^{-2} and is, therefore, consistent with the KSM counting rules, Eq. (8).

-
- [1] G. 't Hooft, Nucl. Phys. **B72**, 461 (1974).
 [2] E. Witten, Nucl. Phys. **B160**, 57 (1979).
 [3] J.L. Gervais and B. Sakita, Phys. Rev. Lett. **52**, 87 (1984); Phys. Rev. D **30**, 1795 (1984); C. Carone, H. Georgi, and S. Osofsky, Phys. Lett. B **322**, 227 (1994); M. Luty and J. March-Russell, Nucl. Phys. **B426**, 71 (1994).
 [4] R. Dashen, E. Jenkins, and A.V. Manohar, Phys. Rev. D **49**, 4713 (1994).
 [5] R. Dashen, E. Jenkins, and A.V. Manohar, Phys. Rev. D **51**, 3697 (1995).
 [6] D.B. Kaplan and M.J. Savage, Phys. Lett. B **365**, 244 (1996).
 [7] D.B. Kaplan and A.V. Manohar, Phys. Rev. C **56**, 76 (1997).
 [8] R. Machleidt, K. Holinde, and Ch. Elster, Phys. Rep. **149**, 1 (1987).
 [9] M.M. Nagels, T.A. Rijken, and J.J. de Swart, Phys. Rev. D **17**, 768 (1978); R. Wiringa, R. Smith, and T. Ainsworth, Phys. Rev. C **29**, 1207 (1984).
 [10] G.S. Adkins, C.R. Nappi, and E. Witten, Nucl. Phys. **B228**, 552 (1983).
 [11] F. Gross, Phys. Rev. **186**, 1448 (1969); Phys. Rev. C **26**, 2203 (1982); *Relativistic Quantum Mechanics and Field Theory* (Wiley, New York, 1993).
 [12] E. Wigner, Phys. Rev. **51**, 106 (1937); **51**, 947 (1937); **56**, 519 (1939).
 [13] S. Weinberg, Phys. Lett. B **251**, 288 (1990); S. Weinberg, Nucl. Phys. **B363**, 3 (1991); C. Ordóñez and U. van Kolck, Phys. Lett. B **291**, 459 (1992); C. Ordóñez, L. Ray, and U. van Kolck, Phys. Rev. Lett. **72**, 1982 (1994); E. Epelbaum, W. Glöckle, and Ulf-G. Meißner, Nucl. Phys. **A637**, 107 (1998); **A671**, 295 (2000).